**Asymptotic preserving space-time discontinuous Galerkin methods for a class of relaxation systems**

by

Anna Lischke

A thesis submitted to the graduate faculty

in partial fulfillment of the requirements for the degree of

MASTER OF SCIENCE

Major: Applied Mathematics

Program of Study Committee:

James A. Rossmanith, Major Professor

Paul Sacks

Jue Yan

Iowa State University

Ames, Iowa

2015

# TABLE OF CONTENTS

# LIST OF TABLES

# LIST OF FIGURES

# ACKNOWLEDGEMENTS

I would like to take this opportunity to express my thanks to those who helped me with various aspects of conducting research and the writing of this thesis. First and foremost, Dr. James Rossmanith for his guidance, patience, and support throughout this research and the writing of this thesis. I would also like to thank my committee members for their efforts and contributions to this work: Dr. Paul Sacks and Dr. Jue Yan. I would additionally like to thank the members of the Department of Mathematics at Iowa State University who have given me their encouragement and support throughout my years as a student at this institution.

# ABSTRACT

Various models derived from the Boltzmann equation can be used to model heat conduction, neutron transport, and gas dynamics. These models arise when one expands the distribution function for the Boltzmann equation in spherical harmonics, which results in singularly perturbed hyperbolic systems scaled by a diffusive relaxation parameter $\varepsilon$. In the diffusive limit where $\varepsilon \ll 1$, the perturbed equations limit to parabolic-type systems such as the heat equation and the advection-diffusion equation. Much work has been done in developing numerical schemes that are useful in the rarefied regime (when $\varepsilon$ is $\mathcal{O}(1)$) and that preserve the diffusive limit (when $\varepsilon \to 0^+$) at the discrete level. A method that does this successfully is called asymptotic preserving (AP).

One difficulty in using standard numerical methods for these models is that they have a very restrictive CFL condition on time-step size which vanishes in the diffusive limit. Some attempts to overcome this hurdle have used implicit time-integration schemes, but this requires computing the solution to very large linear systems at each time step.

Our strategy is to develop a space-time discontinuous Galerkin method that will admit a less restrictive limit on the time-step size and will maintain its order of accuracy as the diffusive relaxation parameter becomes very small.

# CHAPTER 1. INTRODUCTION

The origin of the Boltzmann equation dates back over 100 years, when Maxwell and Boltzmann first devised a method for describing gas states. Since then, the study of the classical Boltzmann equation has presented some difficulty due to the non-linearity of the equation and multi-dimensionality of the distribution function. Hilbert, Chapman, and Enskog developed an approach to deriving transport properties from the Boltzmann equation, which led to the formulation of fluid equations. Fluid equations derived from the Boltzmann equation have been used in a variety of physical applications, including electron transfer in plasma, rarefied gas dynamics, and neutron transport in nuclear reactors [1].

In the context of rarefied gas dynamics, these equations admit a scaling by a diffusive relaxation parameter, the magnitude of which corresponds to that of the mean free path. As the scaling parameter approaches zero, the diffusive scaling leads to Navier-Stokes-type parabolic equations [13]. One difficulty in developing numerical methods for these equations is capturing the macroscopic behavior in the diffusive limit. For the sake of computational tractability, it is better to use schemes which are underresolved in the diffusive limit, i.e., if $\varepsilon$ is the diffusive scaling parameter, the time step ($\Delta t$) and grid size ($\Delta x$) are not required to scale as small as $\mathcal{O}(\varepsilon)$. This leads to the additional difficulty of numerical stiffness, since the CFL limit on the time step size for standard numerical methods is often directly related to $\varepsilon$.

If a numerical scheme remains consistent, stable, and accurate as $\varepsilon \to 0^+$, then the scheme does capture macroscopic behavior of the equations in the diffusive limit, and

the scheme is called asymptotic-preserving [12]. In this thesis, asymptotic-preserving numerical schemes for kinetic equations will be presented and analyzed.

The remainder of the thesis is organized as follows. Sections 1.1 and 1.2 will describe selected kinetic models and how these can be derived from the Boltzmann equation. In Chapter 2, we will introduce discontinuous Galerkin methods in order to provide some background for methods presented in the thesis. In Chapter 3, we define the concept of asymptotic-preservation and describe some methods from the literature which are asymptotic preserving. A new space-time discontinuous Galerkin method will be presented in Chapter 4, followed by numerical results in Chapter 5.

## 1.1 $P_N$ equations

We begin with a form of the Boltzmann radiative-transfer equation in which we assume a distribution of particles moving at a single speed that scatter off a planar background, and which admits a diffusive scaling:

$$\frac{\partial \psi}{\partial t} + \frac{\mu}{\varepsilon}\frac{\partial \psi}{\partial x} = -\frac{\sigma}{\varepsilon^2}\left(\psi - \frac{1}{2}\int_{-1}^{1} \psi(x,\mu,t)\, d\mu\right). \tag{1.1}$$

The unknown function $\psi$ is the density of the particles with respect to the measure $d\mu dx$, $\sigma$ is the scaled material cross-section, $\varepsilon$ is the diffusive scaling parameter corresponding to the mean free path of the particles, and $\mu$ is the cosine of the angle between the direction of travel of a particle and the $x$-axis [9]. We assume that $0 < \varepsilon \leq 1$ and $\psi \in L^2(-1,1)$.

To derive the $P_N$ equations, we expand (1.1) in spherical harmonics. This turns out to be convenient, because the moments of the expansion are the eigenfunctions of the integral collision operator on the right hand side, leading to a relatively simple representation. In one dimension, the spherical harmonics we use in the expansion are Legendre polynomials.

The expansion of the function $\psi$ in (1.1) with Legendre polynomials in terms of the angular variable $\mu$ is

$$\psi(x,\mu,t) = \sum_{k=0}^{N} \frac{2k+1}{2} P_k(\mu)\psi_k(x,t), \tag{1.2}$$

where $P_k(\mu)$ are the Legendre polynomials on the interval $[-1,1]$:

$$P_k \in \left\{1, \mu, \ \frac{1}{2}(3\mu^2-1), \ \frac{1}{2}(5\mu^3-3\mu), ...\right\}, \tag{1.3}$$

and the moments $\psi_k(x,t)$ are defined as

$$\psi_k(x,t) = \int_{-1}^{1} P_k(\mu)\psi(x,\mu,t)\ d\mu. \tag{1.4}$$

We notice that the Legendre polynomials on the interval $[-1,1]$ have the orthogonality property:

$$\int_{-1}^{1} P_i(\mu)P_j(\mu)\ d\mu = \frac{2}{2j+1}\delta_{ij}. \tag{1.5}$$

If we plug the expansion for $\psi$ into (1.1) and integrate against $P_\ell$, we get

$$\begin{aligned}\sum_{k=0}^{N} \frac{2k+1}{2}\left[\psi_{k,t}\int_{-1}^{1} P_kP_\ell\ d\mu + \frac{1}{\varepsilon}\psi_{k,x}\int_{-1}^{1}\mu P_kP_\ell\ d\mu\right] = \\ = \sum_{k=0}^{N}\frac{2k+1}{2}\left(-\frac{\sigma}{\varepsilon^2}\right)\psi_k\left(\int_{-1}^{1}P_kP_\ell\,d\mu - \frac{1}{2}\int_{-1}^{1}P_k\,d\mu\int_{-1}^{1}P_\ell\,d\mu\right).\end{aligned} \tag{1.6}$$

Using the orthogonality property of the Legendre polynomials, this system can be written as

$$\psi_{0,t} + \frac{1}{\varepsilon}\psi_{1,x} = 0, \qquad (\ell = 0), \tag{1.7}$$

$$\psi_{1,t} + \frac{1}{\varepsilon}\frac{\partial}{\partial t}\left[\frac{\ell}{2\ell+1}\psi_{\ell-1} + \frac{\ell+1}{2\ell+1}\psi_{\ell+1}\right] = -\frac{\sigma}{\varepsilon^2}\psi_\ell, \qquad (\ell > 0). \tag{1.8}$$

The system (1.7)-(1.8) is not closed due to the $\psi_{\ell+1}$ term in (1.8). A common way of closing the system is to set $\psi_{N+1} := 0$.

We will restrict our attention to the $P_1$ equations, which can be represented by

$$\psi_{0,t} + \frac{1}{\varepsilon}\psi_{1,x} = 0, \tag{1.9}$$

$$\psi_{1,t} + \frac{1}{3}\frac{1}{\varepsilon}\psi_{0,x} = -\frac{\sigma}{\varepsilon^2}\psi_1. \tag{1.10}$$

We can write the $P_1$ equations in the conservation form

$$\vec{u}_{,t} + A\vec{u}_{,x} = Q_\varepsilon(\psi_0, \psi_1, \sigma), \tag{1.11}$$

where

$$\vec{u} = (\psi_0, \psi_1)^T, \qquad A = \frac{1}{\varepsilon}\begin{pmatrix} 0 & 1 \\ \frac{1}{3} & 0 \end{pmatrix}, \qquad Q_\varepsilon = -\frac{\sigma}{\varepsilon^2}\begin{pmatrix} 0 & 0 \\ 0 & 1 \end{pmatrix}. \tag{1.12}$$

The $P_N$ equations are only used with odd values of $N$ in practice, because the matrix $A$ resulting from using more angular moments has an eigenvalue of 0 for even $N$. This makes it impossible to specify boundary conditions that are consistent with equation (1.1) [9].

Other hyperbolic systems of equations with different integral coupling operators can be derived in a similar way depending on the physics of the transport phenomena being modeled. For the remainder of the thesis, we will assume that $\sigma$ is a constant. A numerical method used to treat the case where $\sigma$ is not constant is described in [9].

## 1.2 Goldstein-Taylor model

A Goldstein-Taylor model [7, 19] can be used to describe the time-evolution of a gas composed of two types of particles moving at equal speeds in opposite directions: one moving in the positive $x$-direction and the other moving in the negative $x$-direction. The equations governing this model can be written with a diffusive scaling as in (1.9)-(1.10), and are given by

$$\begin{aligned} \varepsilon\frac{\partial u}{\partial t} + a\frac{\partial u}{\partial x} &= \frac{1}{\varepsilon}Q_\varepsilon(u, v), \\ \varepsilon\frac{\partial v}{\partial t} - a\frac{\partial v}{\partial x} &= -\frac{1}{\varepsilon}Q_\varepsilon(u, v). \end{aligned} \tag{1.13}$$

The system (1.13) also results from diagonalizing matrix $A$ in (1.12) and letting $u, v$ be the characteristic variables for $\psi_0$ and $\psi_1$. In that case, the characteristic speeds $\pm a$ are $\pm\frac{1}{\varepsilon\sqrt{3}}$.

In (1.13), $u$ is the density of the particles moving parallel to the $x$-axis with velocity $+a$, $v$ is the density of particles moving with velocity $-a$, and $Q_\varepsilon(u,v)$ is the collision operator, which has the form

$$Q_\varepsilon(u,v) = k(u,v)\left(-\alpha_\varepsilon u + \beta_\varepsilon v + \gamma_\varepsilon uv\right). \tag{1.14}$$

The local mass density $\rho$ and the flux $j$ are defined by

$$\rho = u + v \quad \text{and} \quad j = a(u-v)/\varepsilon. \tag{1.15}$$

We can write system (1.13) in terms of the macroscopic variables $\rho$ and $j$ by adding and subtracting the equations.

$$\begin{aligned} \frac{\partial \rho}{\partial t} + \frac{\partial j}{\partial x} &= 0, \\ \varepsilon^2 \frac{\partial j}{\partial t} + a^2 \frac{\partial \rho}{\partial x} &= -2\widehat{Q}_\varepsilon(\rho, j), \end{aligned} \tag{1.16}$$

where

$$\widehat{Q}_\varepsilon(\rho, j) = -\frac{a}{\varepsilon} Q_\varepsilon(u,v). \tag{1.17}$$

For our model problem, we will take

$$k(u,v) = 1, \qquad \alpha_\varepsilon = \beta_\varepsilon = 1, \qquad \gamma_\varepsilon = 0, \qquad a = 1. \tag{1.18}$$

The corresponding equations are [13]

$$\frac{\partial \rho}{\partial t} + \frac{\partial j}{\partial x} = 0, \tag{1.19}$$

$$\varepsilon^2 \frac{\partial j}{\partial t} + \frac{\partial \rho}{\partial x} = -2j. \tag{1.20}$$

In this case, the equations represent the density of particles moving with constant unit speed parallel to the $x$-axis and subject to spontaneous reversals of directions at the jump times of a standard Poisson process of rate 1 [15].

As $\varepsilon \to 0^+$, (1.20) is approximated by

$$\frac{\partial \rho}{\partial x} = -2j, \tag{1.21}$$

the local equilibrium. Combining this with (1.19), we get

$$\frac{\partial \rho}{\partial t} - \frac{1}{2}\frac{\partial^2 \rho}{\partial x^2} = 0, \tag{1.22}$$

the classical heat equation. Hence our hyperbolic system (1.16) is replaced by the parabolic heat equation in the diffusive limit. This is the reason that (1.19)-(1.20) is often called the "hyperbolic heat equation" [12]. For the remainder of the thesis, we will examine numerical methods for the kinetic models presented above.

# CHAPTER 2. DISCONTINUOUS GALERKIN METHODS

This chapter is devoted to a brief history and description of discontinuous Galerkin (DG) methods in order to provide background for the methods presented in this thesis.

DG methods are high-order numerical methods for solving ordinary or partial differential equations (PDEs) with the ability to handle complex geometries and discontinuities in solutions. This makes them particularly well-suited for applications in gas dynamics, viscoelastic flows, oceanography, electro-magnetism, chemical transport, and transport of contaminant in porous media, among others [4, 5]. These are examples of phenomena described by hyperbolic transport equations; however, Bassi and Rebay [3] applied a DG method to purely elliptic problems, and in 1978, Jamet used a scheme which was DG in time to solve parabolic equations [11].

The first DG method was published by Reed and Hill [17] in 1973 and was used for solving the neutron transport equation

$$\sigma u + \nabla \cdot (\mathbf{a}u) = f, \quad \text{in } \Omega, \tag{2.1}$$

where $\sigma$ is a real number and $\mathbf{a}$ is constant vector. The first analysis of this method was produced by LeSaint and Raviart [14], in which they showed the method is optimally $\mathcal{O}(h^{N+1})$ on a Cartesian grid with cell size $h$ and polynomial basis functions of order $N$.

The defining characteristic of DG finite element methods is that they use polynomial representations of the solutions which need not be continuous across cell boundaries, hence the representation of the solution will have discontinuities. Some care must be taken in solving the resulting Riemann problem on the cell boundaries to find the numer-

ical flux. The choice of numerical flux is crucial, as it can affect the scheme's consistency, stability, and accuracy [4, 2].

We will focus our attention on DG schemes for hyperbolic-type equations.

## 2.1 DG methods for 1D hyperbolic systems

We begin with a hyperbolic conservation law in one dimension of the form

$$u_{,t} + Au_{,x} = f(u, t, x), \qquad (t, x) \in \mathbb{R}^+ \times [a, b] \subset \mathbb{R}. \tag{2.2}$$

The function $u : \mathbb{R}^+ \times \mathbb{R}^n \to \mathbb{R}^m$ is the unknown, $Au$ is the flux, and $f$ is the source term. This equation is hyperbolic if the matrix $A$ is diagonalizable with real eigenvalues for all $(t, x) \in [a, b] \times \mathbb{R}^+$.

The first step in developing a DG scheme for this problem is to create spatial grid. We follow the method used in [6]. Let $\Delta x$ be the uniform grid spacing for $m_x$ points in the interval $[a, b]$ (although DG methods can accommodate grids which are not uniform). Then $\Delta x$ is given by

$$\Delta x = \frac{(b - a)}{m_x}. \tag{2.3}$$

We denote the $i^{\text{th}}$ cell (or element) by $\mathcal{T}_i = [x_{i-1/2}, x_{i+1/2}]$, and the cell boundaries are

$$x_{i\pm1/2} = a + (i \pm 1/2)\Delta x, \qquad i = 1, 2, \ldots, m_x. \tag{2.4}$$

The collection of all elements $\mathcal{T}_i$ will be denoted by $\mathcal{T}_h$.

We define our finite element space by

$$V_h := \left\{ v \in L^2([a, b]) \ : \ v\big|_{\mathcal{T}_i} \in P^k, \ \forall \mathcal{T}_i \in \mathcal{T}_h \right\}, \tag{2.5}$$

where $P^k$ represents the space of polynomials of degree at most $n$. Notice that the space $V_h$ contains piecewise-continuous polynomials where no continuity is assumed across the cell boundaries.

Next, we map each element $\mathcal{T}_i$ to the interval $[-1, 1]$ with the affine transformation

$$x = x_i + \xi \frac{\Delta x}{2}. \tag{2.6}$$

For the basis of the polynomial space $P^n$, we will use Legendre polynomials of the form

$$\phi^{(\ell)}(\xi) \in \left\{ 1, \sqrt{3}\xi, \frac{\sqrt{5}}{2}(3\xi^2 - 1), \frac{\sqrt{7}}{2}(5\xi^3 - 3\xi), \dots \right\}, \tag{2.7}$$

which have the orthogonality property

$$\frac{1}{2} \int_{-1}^{1} \phi^{(\ell)}(\xi)\phi^{(k)}(\xi)\, d\xi = \delta_{\ell k}. \tag{2.8}$$

We expand the approximate solution $u_h$ on each element $\mathcal{T}_i$ in terms of the basis functions $\phi^{(\ell)}(\xi)$ to get the *Galerkin expansion* of the form

$$u_h(t, x)\big|_{\mathcal{T}_i} = \sum_{\ell=1}^{M} U^{(\ell)}(t)\phi^{(\ell)}(\xi), \tag{2.9}$$

where $M$ is the desired order of accuracy in space, and the coefficients $U^{(\ell)}(t)$ are computed via the $L^2$ projection

$$U^{(\ell)}(t) = \frac{1}{2} \int_{-1}^{1} u(t, \xi)\phi^{(\ell)}(\xi)\, d\xi. \tag{2.10}$$

Now we are concerned with the evolution of the coefficients $U_i^{(\ell)}(t)$. We multiply both sides of the PDE by the test functions $\phi^{(\ell)}(\xi)$ and integrate over cell $\mathcal{T}_i$, which leads to the semi-discrete variation problem

$$\frac{1}{\Delta x} \int_{-1}^{1} (u_{h,t}(t, \xi) + A u_{h,\xi}(t, \xi))\phi^{(k)}(\xi)\, d\xi = \frac{1}{\Delta x} \int_{-1}^{1} f(u_h, t, \xi)\phi^{(k)}(\xi)\, d\xi. \tag{2.11}$$

We integrate-by-parts to get

$$\begin{aligned} \frac{1}{\Delta x} \int_{-1}^{1} f(u_h, t, \xi)\phi^{(k)}(\xi) d\xi = \frac{1}{\Delta x} \Bigg[ \frac{\partial}{\partial t} \int_{-1}^{1} u_h(t, \xi)\phi^{(k)}(\xi) d\xi \; + A u_h(t, \xi)\phi^{(k)}(\xi) \Big|_{-1}^{1} \\ - \int_{-1}^{1} A u_h(t, \xi)\phi_{\xi}^{(k)}(\xi) d\xi \Bigg]. \end{aligned} \tag{2.12}$$

Then we plug the expansion (2.9) into (2.12) to get a linear system with the unknown vector of coefficients $U^{(\ell)}$. The integral of $f$ against the basis function is usually evaluated with a quadrature rule.

Since $u_h$ is discontinuous across the cell boundaries, we must solve an approximate Riemann problem at $x_{i\pm1/2}$ to define the values of $u_h(t, x_{i\pm1/2})$. A Lax-Friedrichs flux is usually used to approximate the value of $Au_h(t, x_{i\pm1/2})$, although there are other options which preserve the stability and consistency of the scheme. In [2], Arnold and his collaborators present a table of DG methods with their respective appropriate fluxes specified.

In order to describe the flux for one-dimensional, constant-coefficient hyperbolic systems, let us consider the advection equation,

$$u_{,t} + au_{,x} = 0, \qquad (t, x) \in \mathbb{R}^+ \times \mathbb{R}, \tag{2.13}$$

where $a$ is a positive real number and $u : \mathbb{R}^+ \times \mathbb{R} \to \mathbb{R}$. We denote the flux at cell interface $x_{i+1/2}$ by

$$a\hat{u}_{i+1/2}(t) = au_h(t, x_{i+1/2}). \tag{2.14}$$

Since the wave speed $a$ is positive, the advection equation indicates that information propagates from left to right, hence the flux through the left cell boundary $x_{i-1/2}$ should be determined by the value of $u_{h,i-1}(t)$. Therefore, we define the flux as

$$a\hat{u}_{i-1/2}(t) := au_{h,i-1}. \tag{2.15}$$

In other words, we define the value of the approximate solution at the cell interface by its upwind value.

We can extend this fluxing to hyperbolic systems as in (2.2) by diagonalizing the system. Recall that (2.2) is only hyperbolic if the matrix $A$ is diagonalizable with real eigenvalues, so we can decompose $A$ by

$$A = R\Lambda R^{-1}, \tag{2.16}$$

where $R$ is the matrix of right eigenvectors and $\Lambda$ is the diagonal matrix of real eigenvalues. Then we introduce the characteristic variables

$$w = R^{-1}u. \tag{2.17}$$

System (2.2) reduces to

$$w_{,t} + \Lambda w_{,x} = \tilde{f}(w, t, x), \tag{2.18}$$

where

$$\tilde{f}(w, t, x) = R^{-1} f(R^{-1}u, t, x). \tag{2.19}$$

The system (2.18) can be decomposed into a set of decoupled equations with wave speeds $\lambda \in \text{diag}(\Lambda)$. Then we treat each decoupled advection equation in the same way as (2.13).

We have yet to address the matter of the time integration. In the description above, we left $u_h$ continuous in time. The earlier DG methods used Euler or Runge-Kutta methods for time integration, although other difference methods can be used as well [5]. In the following section, we will introduce space-time discontinuous Galerkin methods, in which the finite element solution is integrated against polynomials which vary in both space and time.

## 2.2 Space-time DG methods for 1D hyperbolic systems

To begin formulating a space-time DG method, we must first create a grid in space and time. Each element has the form

$$\mathcal{T}_i^n := [t_n, t_{n+1}] \times [x_{i-1/2}, x_{i+1/2}], \tag{2.20}$$

where $n = 0, \ldots, m_t$ and $i = 1, \ldots, m_x$. We denote the grid spacing in space by $\Delta x$ and in time by $\Delta t$. If $t = 0$ is the initial time and $t = T$ is the final time in the simulation, then

$$\Delta t := \frac{T}{m_t}. \tag{2.21}$$

Next, we map each element $\mathcal{T}_i^n$ to the unit square $[-1,1]\times[-1,1]$ with the transformations

$$x = x_i + \xi\frac{\Delta x}{2}, \qquad\qquad t = t_n + \frac{\Delta t}{2} + \tau\frac{\Delta t}{2}. \tag{2.22}$$

Our finite element space is defined by

$$V_h := \left\{ v \in L^2([0,T]\times[a,b]) \ : \ v\Big|_{\mathcal{T}_i^n} \in P^k, \ \forall \mathcal{T}_i^n \in \mathcal{T}_h \right\}, \tag{2.23}$$

where $P^k$ is the space of Legendre polynomials which vary in space and time:

$$P^k = \text{span}\left(1, \sqrt{3}\xi, \sqrt{3}\tau, 3\xi\tau, \frac{\sqrt{5}}{2}(3\xi^2-1), \frac{\sqrt{5}}{2}(3\tau^2-1), \dots\right). \tag{2.24}$$

For $\psi^{(\ell)}$ and $\psi^{(m)} \in P^k$, we have the orthogonality property

$$\frac{1}{4}\int_{-1}^{1}\int_{-1}^{1} \psi^{(\ell)}(\tau,\xi)\psi^{(m)}(\tau,\xi)\,d\tau d\xi = \delta_{\ell m}. \tag{2.25}$$

Now, the Galerkin expansion has the form

$$u_h(t,x)\Big|_{\mathcal{T}_i^n} = \sum_{\ell=1}^{M(M+1)/2} U_i^{(\ell)n}\psi^{(\ell)}(\tau(t),\xi(x)). \tag{2.26}$$

We arrive at a numerical method for (2.2) by multiplying by a test function $\phi^{(m)}$, integrating over the space-time element, and applying integrations-by-parts on both the $\tau$ and $\xi$ variables. The linear system is given by

$$\begin{aligned} F_{k,i} = &\sum_{\ell=1}^{M(M+1)/2} U_i^{(\ell)n+1}B_{k\ell}^{+} - \sum_{\ell=1}^{M(M+1)/2} U_i^{(\ell)n}B_{k\ell}^{-} + \sum_{\ell=1}^{M(M+1)/2} AU_{i+1}^{(\ell)n}C_{k\ell}^{+} - \\ &- \sum_{\ell=1}^{M(M+1)/2} AU_{i-1}^{(\ell)n}C_{k\ell}^{-} - \sum_{\ell=1}^{M(M+1)/2} U_i^{(\ell)n}D_{k\ell}, \end{aligned} \tag{2.27}$$

where

$$\begin{aligned} B_{k\ell}^{\pm} &= \int_{-1}^{1}\psi^{(k)}(\pm1,\xi)\psi^{(\ell)}(\pm1,\xi)\,d\xi, \\ C_{k\ell}^{\pm} &= \int_{-1}^{1}\psi^{(k)}(\tau,\pm1)\psi^{(\ell)}(\tau,\pm1)\,d\xi, \\ D_{k\ell} &= \int_{-1}^{1}\int_{-1}^{1}\psi^{(k)}(\tau,\xi)(\psi_\tau^{(\ell)} + A\psi_\xi^{(\ell)})\,d\xi d\tau, \\ F_{k,i} &= \int_{-1}^{1}\int_{-1}^{1} f(\tau,\xi)\psi^{(k)}(\tau,\xi)\,d\xi d\tau. \end{aligned} \tag{2.28}$$

We can handle the flux terms which arise from $C^{\pm}$ by upwinding as in the spatial DG method in the previous section. Finally, we solve the linear system for $U_i^{(\ell)n+1}$ for each $\ell$.

# CHAPTER 3. REVIEW OF ASYMPTOTIC PRESERVING SCHEMES

There has been building interest in developing numerical methods for models with a diffusive scaling which preserve the limit system in the discrete sense. Both finite element methods and finite difference methods have been investigated for this purpose, some of which will be described in the following sections. The difficulty with standard numerical methods has been that they require very small time steps in the diffusive limit to maintain stability, resulting in large computational costs as $\varepsilon \to 0^+$.

Shi Jin [12, 13] has achieved success in developing an AP scheme for the hyperbolic heat equation by utilizing an operator splitting method with a semi-implicit finite difference for the time discretization and an explicit finite difference for the spatial discretization. However, this method has a maximum time-step restriction and reduces to second order in the diffusive limit.

McClarren, Evans, Lowrie, and Densmore [16] have developed an AP scheme for the $P_N$ equations using a semi-implicit time-integration method in combination with a discontinuous Galerkin spatial discretization. Their scheme also has a maximum time step restriction, but it relaxes in the diffusive limit due to the properties of the DG method.

The finite volume method for the hyperbolic heat equation by Gosse and Toscani [8] is also asymptotic preserving, but this method is much less accurate in the rarefied regime.

We will describe and analyze these methods in detail and compare them with our

space-time DG method.

## 3.1 Definition of asymptotic preserving

In order for a scheme to be asymptotic preserving (AP), it must be consistent with the partial differential equation in both the rarefied regime and in the diffusive limit. This is described in the Figure 3.1

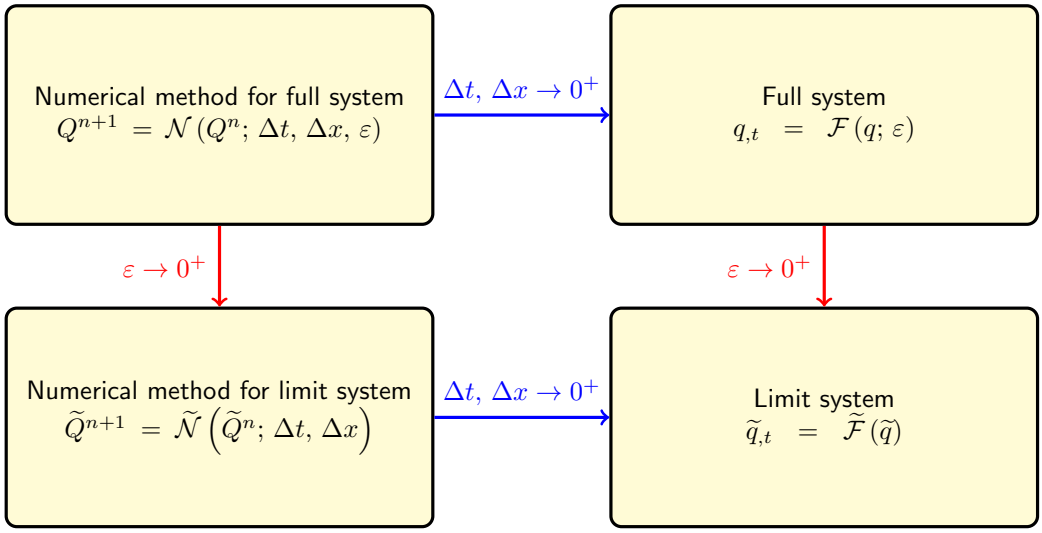


Figure 3.1 Asymptotic preserving numerical methods

If our numerical scheme is asymptotic preserving, we should get the limit to the full hyperbolic system if we fix $\varepsilon$ and refine the mesh. Then if we take $\varepsilon \to 0^+$, the solution should limit to the solution of the parabolic limit system. Likewise, if we first fix $\Delta t$ and $\Delta x$ and take $\varepsilon \to 0^+$, the result should be a valid numerical method for the limit system, and as we refine the mesh, we should get the solution of the limit system.

## 3.2 AP operator splitting scheme

If we use standard explicit finite difference schemes for the Goldstein-Taylor equations (1.19)-(1.20) directly, we will get a CFL limit that requires $\Delta t$ to scale like $\varepsilon^2$ when

$\Delta x \gg \varepsilon$. In fact, the limit for $\Delta t$ is given by

$$\Delta t \leq \min(\varepsilon \Delta x, \varepsilon^2). \tag{3.1}$$

This is undesirable because in the diffusive regime, we would like to have $\Delta t, \Delta x \gg \varepsilon$ in order for the scheme to be asymptotic preserving.

Jin, Pareschi, and Toscani [13] introduced an AP finite difference scheme for the system (1.19)-(1.20) which incorporated an operator splitting approach. We present their scheme below. The key idea for this approach is to separate the system into "stiff" and "non-stiff" pieces and numerically solve these pieces independently.

First, we reformulate system (1.19)-(1.20) as

$$\frac{\partial \rho}{\partial t} + \frac{\partial j}{\partial x} = 0, \tag{3.2}$$

$$\frac{\partial j}{\partial t} + \frac{\partial \rho}{\partial x} = -\frac{2}{\varepsilon^2}\left[j + \frac{1-\varepsilon^2}{2}\frac{\partial \rho}{\partial x}\right]. \tag{3.3}$$

We separate this system into a "collision" step

$$\frac{\partial \rho}{\partial t} = 0, \tag{3.4}$$

$$\frac{\partial j}{\partial t} = -\frac{2}{\varepsilon^2}\left[j + \frac{1-\varepsilon^2}{2}\frac{\partial \rho}{\partial x}\right], \tag{3.5}$$

and a "convection" step

$$\frac{\partial \rho}{\partial t} + \frac{\partial j}{\partial x} = 0, \tag{3.6}$$

$$\frac{\partial j}{\partial t} + \frac{\partial \rho}{\partial x} = 0. \tag{3.7}$$

For the collision step we use an implicit backward Euler time discretization, and an explicit scheme for the convection step. At first, we leave the spatial derivatives continuous. The discretization is done as follows

$$\begin{aligned} &\rho^* - \rho^n = 0, \\ &\frac{j^* - j^n}{\Delta t} = -\frac{2}{\varepsilon^2}\left[j^* + \frac{1-\varepsilon^2}{2}\rho_x^*\right], \end{aligned} \tag{3.8}$$

$$\begin{aligned} \frac{\rho^{n+1}-\rho^n}{\Delta t} + j^*_{,x} &= 0, \\ \frac{j^{n+1}-j^*}{\Delta t} + \rho^*_{,x} &= 0. \end{aligned} \tag{3.9}$$

The terms $\rho^*$ and $j^*$ are used as intermediate solutions to link the two steps. The spatial discretizations are taken independently. If we solve for $\rho^*$ and $j^*$ and plug these into the second step, the resulting scheme is

$$\begin{aligned} \frac{\rho^{n+1}-\rho^n}{\Delta t} + \frac{1}{1+2\frac{\Delta t}{\varepsilon^2}} j^n_{,x} &= (1-\varepsilon^2)\frac{\frac{\Delta t}{\varepsilon^2}}{1+2\frac{\Delta t}{\varepsilon^2}}\rho^n_{,x,x}, \\ \frac{j^{n+1}-j^n}{\Delta t} + \left[1+\frac{(1-\varepsilon^2)\frac{1}{\varepsilon^2}}{1+2\frac{\Delta t}{\varepsilon^2}}\right]\rho^n_{,x} &= -\frac{\frac{2}{\varepsilon^2}}{1+2\frac{\Delta t}{\varepsilon^2}} j^n. \end{aligned} \tag{3.10}$$

By defining the parameters $\alpha$, $\beta$, $\gamma$, and $\delta$:

$$\begin{aligned} \alpha &= \frac{1}{1+2\frac{\Delta t}{\varepsilon^2}}, \\ \beta &= 1+\frac{(1-\varepsilon^2)\frac{1}{\varepsilon^2}}{1+2\frac{\Delta t}{\varepsilon^2}}, \\ \gamma &= (1-\varepsilon^2)\frac{\frac{\Delta t}{\varepsilon^2}}{1+2\frac{\Delta t}{\varepsilon^2}}, \\ \delta &= \frac{\frac{2}{\varepsilon^2}}{1+2\frac{\Delta t}{\varepsilon^2}}, \end{aligned} \tag{3.11}$$

the time discretization is consistent with the hyperbolic system

$$\begin{aligned} \rho_{,t} + \alpha j_{,x} &= \gamma \rho_{,xx}, \\ j_{,t} + \beta \rho_{,x} &= -\delta j. \end{aligned} \tag{3.12}$$

Jin *et al.* then use a van Leer second order upwind scheme with slope limiters for the convection terms and a central difference for the diffusion term to do the spatial discretization.

$$\begin{aligned} \frac{\rho_i^{n+1}-\rho_i^n}{\Delta t} =& -\frac{\alpha}{2\Delta x}(j^n_{i+1}-j^n_{i-1}) + \frac{\sqrt{\alpha\beta}}{2\Delta x}(\rho^n_{i+1}-2\rho^n_i+\rho^n_{i-1}) \\ & - \frac{\sqrt{\alpha\beta}}{4}(\sigma^-_{i+1}-\sigma^+_i-\sigma^-_i+\sigma^+_{i-1}) - \delta j^n_i, \\ \frac{j_i^{n+1}-j^n}{\Delta t} =& -\frac{\beta}{2\Delta x}(\rho^n_{i+1}-\rho^n_{i-1}) + \frac{\sqrt{\alpha\beta}}{2\Delta x}(j^n_{i+1}-2j^n+j^n_{i-1}) \\ & + \frac{\beta}{4}(\sigma^-_{i+1}-\sigma^+_i-\sigma^-_i+\sigma^+_{i-1}) - \delta j^n_x, \end{aligned} \tag{3.13}$$

where $\sigma_i^{\pm}$ are the slopes of the Riemann invariants on the $i^{\text{th}}$ cell:

$$\begin{aligned}
\sigma_i^{\pm} &= \frac{1}{\Delta x}\left(\rho_{i+1} \pm \sqrt{\frac{\alpha}{\beta}} j_{i+1} - \rho_i \mp \sqrt{\frac{\alpha}{\beta}} j_i\right) \psi(\theta_i^{\pm}), \\
\theta_i^{\pm} &= \left[\frac{\rho_i^n \pm \sqrt{\frac{\alpha}{\beta}} j_i - \rho_{i-1}^n \mp \sqrt{\frac{\alpha}{\beta}} j_{i-1}}{\rho_{i+1}^n \pm \sqrt{\frac{\alpha}{\beta}} j_{i+1} - \rho_i^n \mp \sqrt{\frac{\alpha}{\beta}} j_i}\right], \\
\psi(\theta) &= \frac{|\theta| + \theta}{1 + |\theta|}.
\end{aligned} \tag{3.14}$$

Other slope-limiter functions $\psi$ are permissible as long as they satisfy

$$0 \leq \frac{\psi(\theta)}{\theta} \leq 2, \tag{3.15}$$

so that the scheme remains total variation-decreasing (TVD).

The stability condition

$$\frac{\Delta t}{\Delta x^2} \leq \frac{1}{4} \tag{3.16}$$

ensures the stability of the scheme for all $\varepsilon$ such that $0 < \varepsilon \leq 1$. Since $\varepsilon$ does not appear in the CFL condition, the choice of $\Delta t$ is independent of $\varepsilon$. This is important for asymptotic preservation. Also, as we take the limit as $\varepsilon \to 0^+$, we find that the numerical scheme limits to

$$\frac{\rho_i^{n+1} - \rho_i^n}{\Delta t} = \frac{1}{2\Delta x^2}(\rho_{i+1}^n - 2\rho_i^n + \rho_{i-1}^n), \tag{3.17}$$

which is consistent with the limiting heat equation. This shows that the scheme is indeed asymptotic-preserving.

A drawback to this method is that as $\varepsilon \to 0^+$, in order to satisfy the condition (3.16) in the diffusive limit, $\Delta t$ must scale like $\Delta x^2$. This an artifact of the splitting itself, and is not overcome by using alternate discretizations.

This method can be used for other diffusively scaled kinetic equations, such as the Ruijgrok-Wu model [18] which limits to the Burgers equation, or the Carleman model, which limits to the porous medium equation [12]. A second order Strang splitting may also be used in place of the first order splitting described above in order to achieve second order accuracy in time.

## 3.3 AP semi-implicit DG scheme

An AP DG method for the $P_N$ equations was devised by McClarren, Evans, Lowrie, and Densmore in [16]. This method relies on the properties of the DG method itself instead of a splitting of the PDE to achieve asymptotic preservation. The time integration is carried out using a predictor-corrector method which is equivalent to a second-order Runge-Kutta method for the convection terms and a backward Euler method for the coupling terms. They use a second order DG method for the spatial discretization, which becomes equivalent to a continuous finite element method in the diffusive limit. The CFL limit for this method requires that $\Delta t \sim \Delta x^2$.

We will focus our description of the method on the $P_1$ equations, which can be written in conservation form as in (1.11):

$$u_{,t} + Au_{,x} = Q_\varepsilon u, \tag{3.18}$$

where

$$u = \begin{pmatrix} \psi_0 \\ \psi_1 \end{pmatrix}, \qquad A = \frac{1}{\varepsilon}\begin{pmatrix} 0 & 1 \\ \frac{1}{3} & 0 \end{pmatrix}, \qquad Q_\varepsilon = -\frac{\sigma}{\varepsilon^2}\begin{pmatrix} 0 & 0 \\ 0 & 1 \end{pmatrix}. \tag{3.19}$$

We will need the eigensystem of $A$, which is given by

$$A = R\Lambda R^{-1}. \tag{3.20}$$

Here, $R$ is the matrix of eigenvectors, and $\Lambda$ is the diagonal matrix of eigenvalues of $A$. In the case of the $P_1$ equations, the decomposition can be written as

$$A = \begin{pmatrix} -\sqrt{3} & \sqrt{3} \\ 1 & 1 \end{pmatrix}\begin{pmatrix} -\frac{1}{\sqrt{3}} & 0 \\ 0 & \frac{1}{\sqrt{3}} \end{pmatrix}\begin{pmatrix} -\frac{1}{2\sqrt{3}} & \frac{1}{2} \\ \frac{1}{2\sqrt{3}} & \frac{1}{2} \end{pmatrix}. \tag{3.21}$$

We introduce the notation $|\Lambda|$ to mean the matrix of the absolute values of the elements of $\Lambda$. Then

$$|A| := R|\Lambda|R^{-1} = \begin{pmatrix} \frac{\sqrt{3}}{3} & 0 \\ 0 & \frac{\sqrt{3}}{3} \end{pmatrix}. \tag{3.22}$$

We will discretize the domain $[0,T]\times[a,b]$ in time and space as in (2.20), where $\Delta t$ is the time step size and $\Delta x$ is the spatial grid size, where we assume a uniform mesh. Now we can describe the time integration procedure used in [16]. The predictor step is given by

$$u^{n+1/2}-\frac{\Delta t}{2}Q_\varepsilon u^{n+1/2}=u^n-\frac{\Delta t}{2}A\frac{du}{dx}\bigg|_n, \tag{3.23}$$

where $u^n=u(x,n\Delta t)$, and the corrector step is

$$u^{n+1}-\Delta t Q_\varepsilon u^{n+1}=u^n-\Delta t A\frac{du}{dx}\bigg|_{n+1/2}. \tag{3.24}$$

The convection terms are treated with a second order Runge Kutta method, and the source terms are treated with a first order backward Euler method.

We spatially discretize (1.11) with a DG method using linear polynomial approximations, which should result in a second order accurate method in space. We first multiply (1.11) by a basis function $B_{ki}$ and integrate over cell $\mathcal{T}_k$. Then we have

$$\partial_t\int_{\mathcal{T}_k}B_{ki}u\,dx+A[B_{ki}u]_{x_{k-1/2}}^{x_{k+1/2}}-A\int_{\mathcal{T}_k}u\partial_x B_{ki}\,dx=\int_{\mathcal{T}_k}B_{ki}Q_\varepsilon u\,dx. \tag{3.25}$$

We expand the unknown $u$ in terms of the basis polynomials $B_{ki}$ by

$$u(x,t)=\sum_{k=1}^{m_x}\sum_{j=1}^{M}u_{kj}(t)B_{kj}(x), \tag{3.26}$$

where $m_x$ is the number of spatial cells and $M$ is the desired order of accuracy. We also expand $Q_\varepsilon$ in the same way. For this method, $M=2$, since the basis function $B_{kj}$ are linear. If we substitute this expansion into (3.25), we get 2 ordinary differential equations per cell in terms of $u_{kj}$. For the cell $\mathcal{T}_k$, we have

$$M_{kij}\frac{d}{dt}u_{kj}+A[B_{ki}u]_{x_{k-1/2}}^{x_{k+1/2}}-K_{kij}Au_{kj}=M_{kij}Q_\varepsilon u_{kj},\qquad 1\le i\le 2, \tag{3.27}$$

where

$$M_{kij}=\int_{\mathcal{T}_k}B_{ki}B_{kj}\,dx,\qquad K_{kij}=\int_{\mathcal{T}_k}B_{kj}\partial_x B_{ki}\,dx. \tag{3.28}$$

We will then sum over the subscript $j$. The flux on the boundaries should be chosen in order to ensure conservation. For equation (1.11), we will need to use the same value for $Au_{k+1/2}$ for cell $k$ and $k+1$. The left boundary value from cell $k$ will be denoted by $u^L_{k+1/2}$ and the right boundary value will be denoted by $u^R_{k+1/2}$.

$$Au_{k+1/2} = A\overline{u}_{k+1/2} - \frac{1}{2}|A|\Delta u_{k+1/2}, \tag{3.29}$$

where

$$\overline{u}_{k+1/2} = \frac{1}{2}(u^L_{k+1/2} + u^R_{k+1/2}), \tag{3.30}$$

$$\Delta u_{k+1/2} = u^R_{k+1/2} - u^L_{k+1/2}, \tag{3.31}$$

$$|A| = R|\Lambda|R^{-1}. \tag{3.32}$$

This is an upwind flux in the sense that positive eigenvalues of $A$ indicate that information propagates from left to right, and negative eigenvalues indicate propagation from right to left. For the $P_1$ equations, we get

$$Au_{k+1/2} = \frac{1}{\varepsilon}\begin{pmatrix} \overline{\psi}_1 \\ \frac{1}{3}\overline{\psi}_0 \end{pmatrix}_{k+1/2} - \frac{1}{2\varepsilon\sqrt{3}}\begin{pmatrix} \Delta\psi_0 \\ \Delta\psi_1 \end{pmatrix}_{k+1/2}. \tag{3.33}$$

We define our linear basis function $B_{k,i}$ by

$$B_{k1}(x) = \frac{x_k + \frac{\Delta x}{2} - x}{\Delta x}, \qquad B_{k2}(x) = \frac{x - x_k + \frac{\Delta x}{2}}{\Delta x}. \tag{3.34}$$

If we plug in our flux and evaluate the integrals of these basis functions, we get the linear system

$$M_{kij}\frac{d}{dt}u_{kj} + \delta_{i2}(Au)_{k+1/2} - \delta_{i1}(Au)_{k-1/2} - K_{kij}Au_{kj} = M_{kij}Q_\varepsilon u_{kj}, \quad i = 1, 2, \tag{3.35}$$

where

$$M_k = \frac{\Delta x}{6}\begin{pmatrix} 2 & 1 \\ 1 & 2 \end{pmatrix}, \quad K_k = \frac{1}{2}\begin{pmatrix} -1 & -1 \\ 1 & 1 \end{pmatrix}, \tag{3.36}$$

$$\delta_{i1} = \begin{pmatrix} 1 \\ 0 \end{pmatrix}, \quad \delta_{i2} = \begin{pmatrix} 0 \\ 1 \end{pmatrix}.$$

If we multiply (3.35) through by $M_k^{-1}$, we get

$$\frac{d}{dt}u_{k1} + \frac{-2(Au)_{k+1/2} - 4(Au)_{k-1/2} + 3A(u_{k1}+u_{k2})}{\Delta x} = Q_\varepsilon u_{k1}, \tag{3.37}$$

$$\frac{d}{dt}u_{k2} + \frac{2(Au)_{k-1/2} + 4(Au)_{k+1/2} - 3A(u_{k1}+u_{k2})}{\Delta x} = Q_\varepsilon u_{k2}. \tag{3.38}$$

We can see that conservation is indeed preserved by this method by adding these two equations. Indeed,

$$\frac{1}{2}\frac{d}{dt}(u_{k1}+u_{k2}) + \frac{(Au)_{k+1/2} - (Au)_{k-1/2}}{\Delta x} = \frac{1}{2}(Q_\varepsilon u_{k1} + Q_\varepsilon u_{k2}). \tag{3.39}$$

Now we combine the spatial and temporal discretizations to get the following predictor-corrector method. The predictor step is

$$\frac{u_{k1}^{n+1/2} - u_{k1}^n}{\Delta t/2} + \frac{-2(Au)_{k+1/2}^n - 4(Au)_{k-1/2}^n + 3A(u_{k1}^n + u_{k2}^n)}{\Delta x} = Q_\varepsilon u_{k1}^{n+1/2}, \tag{3.40}$$

$$\frac{u_{k2}^{n+1/2} - u_{k2}^n}{\Delta t/2} + \frac{2(Au)_{k-1/2}^n + 4(Au)_{k+1/2}^n - 3A(u_{k1}^n + u_{k2}^n)}{\Delta x} = Q_\varepsilon u_{k2}^{n+1/2}. \tag{3.41}$$

The corrector step is

$$\frac{u_{k1}^{n+1} - u_{k1}^n}{\Delta t} + \frac{-2(Au)_{k+1/2}^{n+1/2} - 4(Au)_{k-1/2}^{n+1/2} + 3A(u_{k1}^{n+1/2} + u_{k2}^{n+1/2})}{\Delta x} = Q_\varepsilon u_{k1}^{n+1}, \tag{3.42}$$

$$\frac{u_{k2}^{n+1} - u_{k2}^n}{\Delta t} + \frac{2(Au)_{k-1/2}^{n+1/2} + 4(Au)_{k+1/2}^{n+1/2} - 3A(u_{k1}^{n+1/2} + u_{k2}^{n+1/2})}{\Delta x} = Q_\varepsilon u_{k2}^{n+1}. \tag{3.43}$$

In the rarefied regime ($\varepsilon \sim \mathcal{O}(1)$), the time step for this method is limited by the CFL condition

$$\frac{\Delta t}{\varepsilon \Delta x} \leq \frac{1}{3}. \tag{3.44}$$

As $\varepsilon \to 0^+$, the CFL condition relaxes to

$$\frac{1}{3\sigma\Delta x}\frac{\Delta t}{\varepsilon\Delta x} \leq \frac{1}{6}. \tag{3.45}$$

In the diffusion limit, the $\sigma\Delta x$ term is scaled like $\mathcal{O}(\varepsilon^{-1})$, so $\Delta t$ is not forced to scale with $\varepsilon$. One of the key ingredients that makes this method is successful is the fact that as $\varepsilon \to 0^+$, for each $k$,

$$u^R_{k+1/2} = u^L_{k+1/2}, \tag{3.46}$$

so the DG method becomes a continuous finite element method. This is consistent with the behavior of the parabolic-type limit equation because the discontinuities in the representation of the solution will be smoothed. This method can be generalized for the $P_N$ equations where $N > 1$ as well.

This method avoids the splitting error inherent in the scheme by Shi Jin [12] presented in Section 3.2, however, there is still a strict CFL limit for the scheme, albeit less restrictive in the diffusive regime. But the fact that the AP quality is preserved due to the properties of the DG method itself gives hope that progress might be made toward an unconditionally stable scheme by using an approach along these lines.

## 3.4 AP finite volume method

Gosse and Toscani [8] developed a third type of numerical method for the one-dimensional Goldstein-Taylor model (1.13), in which they applied a finite volume method to achieve an asymptotic preserving scheme. This is an example of a "well-balanced" scheme, which means that the derivation depends on a localization of the source terms by a Dirac delta function. This method does not involve any operator splitting or finite elements, and the CFL condition in the diffusive limit is $\Delta t < \sigma\Delta x^2$.

Recall the Goldstein-Taylor model given by

$$\begin{aligned} \frac{\partial w_1}{\partial t} + \frac{1}{\varepsilon}\frac{\partial w_1}{\partial x} &= \frac{1}{\varepsilon^2}(w_2 - w_1), \\ \frac{\partial w_2}{\partial t} - \frac{1}{\varepsilon}\frac{\partial w_2}{\partial x} &= \frac{1}{\varepsilon^2}(w_1 - w_2), \end{aligned} \tag{3.47}$$

where $0 < \varepsilon \leq 1$. We modify the collision terms with a localization that concentrates the effects of the collision operator on the cell boundaries:

$$\begin{aligned} \frac{\partial w_1}{\partial t} + \frac{\partial w_1}{\partial x} &= \frac{\sigma \Delta x}{2\varepsilon^2} \sum_{j \in \mathbb{Z}} (w_2 - w_1)\delta(x - x_{j-1/2}), \\ \frac{\partial w_2}{\partial t} - \frac{\partial w_2}{\partial x} &= \frac{\sigma \Delta x}{2\varepsilon^2} \sum_{j \in \mathbb{Z}} \Delta x (w_1 - w_2)\delta(x - x_{j-1/2}). \end{aligned} \tag{3.48}$$

These Dirac masses induce a static wave which results in a more complicated Riemann problem. For initial data $(w_{1L}, w_{1R})$ and $(w_{2L}, w_{2,R})$, and with a jump at $x = x_{j-1/2}$,

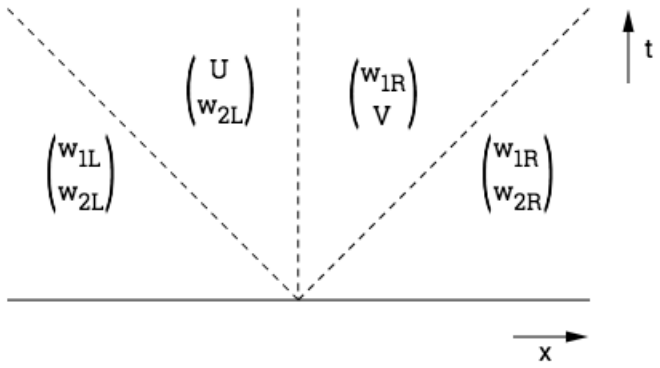


Figure 3.2 Riemann problem with stationary wave

we wish to solve for $U$ and $V$ in the Riemann problem:

$$\begin{cases} (w_{1L}, w_{2L}), & \text{for } x - x_{j-1/2} < -t, \\ (w_{1L}, V), & \text{for } x - x_{j-1/2} \in (-t, 0), \\ (U, w_{2R}), & \text{for } x - x_{j-1/2} \in (0, t), \\ (w_{1R}, w_{2R}), & \text{for } x - x_{j-1/2} > t. \end{cases} \tag{3.49}$$

Along the stationary wave, we have the jump condition

$$U - w_{1R} = \frac{\sigma \Delta x}{2\varepsilon}(w_{2L} - U), \tag{3.50}$$

$$V - w_{2L} = \frac{\sigma \Delta x}{2\varepsilon}(w_{1R} - V). \tag{3.51}$$

Solving for $U$ and $V$ gives

$$U = w_{2L} + \frac{2\varepsilon}{\sigma \Delta x + 2\varepsilon}(w_{1R} - w_{2L}), \tag{3.52}$$

$$V = w_{1R} + \frac{2\varepsilon}{\sigma \Delta x + 2\varepsilon}(w_{2L} - w_{1R}). \tag{3.53}$$

$$\tag{3.54}$$

The addition of the static wave at the cell boundary leads to a non-conservative formulation of the PDE, which means that the fluxes on either side of the same cell boundary may not be equal. Hence at the cell boundary $x_{j-1/2}$, we define the left and right fluxes

$$F^-_{j-1/2} = \frac{1}{\varepsilon} \begin{pmatrix} -U_{j-1/2} \\ w_{2j-1} \end{pmatrix}, \tag{3.55}$$

$$F^+_{j-1/2} = \frac{1}{\varepsilon} \begin{pmatrix} -w_{1j} \\ V_{j-1/2} \end{pmatrix}. \tag{3.56}$$

The finite volume method has the form

$$W_i^{n+1} = W_i^n - \frac{\Delta t}{\Delta x}(F^-_{j+1/2} - F^+_{j-1/2}). \tag{3.57}$$

Plugging in the fluxes and updating the convection terms implicitly results in the scheme:

$$\begin{aligned} W_{1j}^{n+1} - \frac{\Delta t}{\varepsilon \Delta x}(W_{1j+1}^{n+1} - W_{1j}^{n+1}) &= W_{1j}^n + \frac{2\Delta t}{\Delta x(\sigma \Delta x + 2\varepsilon)}(W_{1j+1}^n - W_{2j}^n), \\ W_{2j}^{n+1} + \frac{\Delta t}{\varepsilon \Delta x}(W_{2j}^{n+1} - W_{2j-1}^{n+1}) &= W_{2j}^n - \frac{2\Delta t}{\Delta x(\sigma \Delta x + 2\varepsilon)}(W_{1j}^n - W_{2j-1}^n). \end{aligned} \tag{3.58}$$

Now we assume that the terms $|W_{1j+1}^n - W_{2j}^n|$ and $|W_{1j}^n - W_{2j-1}^n|$ are $\mathcal{O}(\varepsilon)$. This is done in order to ensure the scheme behaves nicely in the diffusive limit. With this assumption,

as $\varepsilon \to 0^+$,

$$\begin{aligned} W_{1j+1}^n &\to W_{2j}^n, \\ W_{2j-1}^n &\to W_{1j}^n. \end{aligned} \tag{3.59}$$

Then we can replace $W_{1j+1}^{n+1}$ and $W_{2j-1}^{n+1}$ in (3.58) with their respective limits (3.59) to get

$$\begin{aligned} W_{1j}^{n+1} - \frac{\Delta t}{\varepsilon \Delta x}(W_{2j}^{n+1} - W_{1j}^{n+1}) &= W_{1j}^n + \frac{2\Delta t}{\Delta x(\sigma \Delta x + 2\varepsilon)}(W_{1j+1}^n - W_{2j}^n), \\ W_{2j}^{n+1} + \frac{\Delta t}{\varepsilon \Delta x}(W_{2j}^{n+1} - W_{1j}^{n+1}) &= W_{2j}^n - \frac{2\Delta t}{\Delta x(\sigma \Delta x + 2\varepsilon)}(W_{1j}^n - W_{2j-1}^n). \end{aligned} \tag{3.60}$$

If we add both equations in (3.60) and define $\rho_j^{n+1} = W_{1j}^{n+1} + W_{2j}^{n+1}$, we get the scheme:

$$\begin{aligned} \rho_j^{n+1} = \rho_j^n &+ \frac{\Delta t}{\sigma \Delta x^2}(\rho_{j+1}^n - 2\rho_j^n + \rho_{j-1}^n) \\ &+ \frac{\Delta t}{\Delta x(\sigma \Delta x + 2\varepsilon)} \left[ W_{2j+1}^n - W_{1j+1}^n + W_{2j-1}^n - W_{1j-1}^n - \varepsilon \frac{\rho_{j+1}^n - 2\rho_j^n + \rho_{j-1}^n}{\Delta x} \right]. \end{aligned} \tag{3.61}$$

This discretization matches that of the heat equation in the diffusive limit as in (1.22) with some added physical dissipation under that assumption that $|W_{1j}^n - W_{2j}^n| = \mathcal{O}(\varepsilon)$.

This method is stable if the CFL condition $\Delta t < \sigma \Delta x^2$ is satisfied, and it preserves the macroscopic behavior of the diffusive limit system well. However, in the rarefied regime, this method is not very accurate, mostly due to the assumption made in (3.59). So if one is interested in a truly AP method, the schemes by Jin [13, 12] and McClarren [16] perform better, because they model the behavior of the true solution more closely for both large and small values of $\varepsilon$.

# CHAPTER 4. AP SPACE-TIME DG METHOD

Below we develop an asymptotic preserving space-time discontinuous Galerkin method for the hyperbolic heat equation

$$\begin{aligned} \rho_{,t} + u_{,x} &= 0, \\ u_{,t} + \frac{1}{\varepsilon^2}\rho, x &= -\frac{\sigma}{\varepsilon^2}u. \end{aligned} \tag{4.1}$$

We will work with the characteristic form of the system,

$$\begin{aligned} w_{1,t} - \frac{1}{\varepsilon}w_{1,x} &= \frac{\sigma}{2\varepsilon^2}(w_2 - w_1), \\ w_{2,t} + \frac{1}{\varepsilon}w_{2,x} &= \frac{\sigma}{2\varepsilon^2}(w_1 - w_2), \end{aligned} \tag{4.2}$$

where

$$\begin{aligned} \rho &= w_1 + w_2, \\ u &= \frac{1}{\varepsilon}(w_2 - w_1). \end{aligned} \tag{4.3}$$

We map the independent variables, $\tau \in [-1, 1]$ and $\xi \in [-1, 1]$ on the space-time mesh element

$$\mathcal{T}_i^{n+1} := [t^n, t^{n+1}] \times \left[x_i - \frac{\Delta x}{2}, x_i + \frac{\Delta x}{2}\right], \tag{4.4}$$

with the affine transformations

$$x = x_i + \xi\left(\frac{\Delta x}{2}\right) \qquad \text{and} \qquad t = \frac{1}{2}(t^n + t^{n+1}) + \tau\left(\frac{\Delta t}{2}\right). \tag{4.5}$$

In these variables, the system (4.2) become

$$w_{1,\tau} - \nu w_{1,\xi} = \frac{\alpha}{2}(w_2 - w_1), \tag{4.6}$$

$$w_{2,\tau} + \nu w_{2,\xi} = \frac{\alpha}{2}(w_1 - w_2), \tag{4.7}$$

where

$$\nu = \frac{\Delta t}{\varepsilon \Delta x} \qquad \text{and} \qquad \alpha = \frac{\sigma \Delta t}{2\varepsilon^2} = \frac{\sigma \nu \Delta x}{2\varepsilon}. \tag{4.8}$$

In the space-time DG method, we assume the following ansatz on each element:

$$w_k\Big|_{\mathcal{T}_i^{n+1}} = \sum_{\ell=1}^{M(M+1)/2} W_{ki}^{(\ell)n+1} \psi^{(\ell)}(\tau, \xi), \qquad k = 1, 2, \tag{4.9}$$

where $M$ is the desired order of accuracy in both space and time, and

$$\psi^{(\ell)}(\tau, \xi) \in \left\{ 1, \sqrt{3}\xi, \sqrt{3}\tau, 3\tau\xi, \frac{\sqrt{5}}{2}(3\xi^2 - 1), \frac{\sqrt{5}}{2}(3\tau^2 - 1), \dots \right\} \tag{4.10}$$

are orthogonal basis polynomials on $(\tau, \xi) \in [-1, 1] \times [-1, 1]$, with the orthogonality property:

$$\frac{1}{4} \int_{-1}^{1} \int_{-1}^{1} \psi^{(\ell)}(\tau, \xi) \psi^{(k)}(\tau, \xi) \, d\tau \, d\xi = \delta_{\ell k}. \tag{4.11}$$

We arrive at a numerical method for system (4.2) by multiplying by a test function $\psi^{(k)}$, integrating over the space-time element, and applying integrations-by-parts on both the $\tau$ and $\xi$ variables:

$$\begin{aligned}
&\sum_{\ell=1}^{M(M+1)/2} \left[ A_{k\ell}^{+} W_{1i}^{(\ell)n+1} - A_{k\ell}^{-} W_{1i}^{(\ell)n} - \nu B_{k\ell}^{+} W_{1i+1}^{(\ell)n+1} + \nu B_{k\ell}^{-} W_{1i}^{(\ell)n+1} \right] \\
&\qquad - \sum_{\ell=1}^{M(M+1)/2} D_{k\ell}^{-} W_{1i}^{(\ell)n+1} = \alpha \left( W_{2i}^{(k)n+1} - W_{1i}^{(k)n+1} \right), \\
&\sum_{\ell=1}^{M(M+1)/2} \left[ A_{k\ell}^{+} W_{2i}^{(\ell)n+1} - A_{k\ell}^{-} W_{2i}^{(\ell)n} + \nu C_{k\ell}^{+} W_{2i}^{(\ell)n+1} - \nu C_{k\ell}^{-} W_{2i-1}^{(\ell)n+1} \right] \\
&\qquad - \sum_{\ell=1}^{M(M+1)/2} D_{k\ell}^{+} W_{2i}^{(\ell)n+1} = \alpha \left( W_{1i}^{(k)n+1} - W_{2i}^{(k)n+1} \right),
\end{aligned} \tag{4.12}$$

where

$$A_{k\ell}^{\pm} = \frac{1}{2}\int_{-1}^{1} \psi^{(k)}(\pm 1,\xi)\psi^{(\ell)}(\pm 1,\xi)\, d\xi, \tag{4.13}$$

$$B_{k\ell}^{\pm} = \frac{1}{2}\int_{-1}^{1} \psi^{(k)}(\tau,\pm 1)\psi^{(\ell)}(\tau,-1)\, d\tau, \tag{4.14}$$

$$C_{k\ell}^{\pm} = \frac{1}{2}\int_{-1}^{1} \psi^{(k)}(\tau,\pm 1)\psi^{(\ell)}(\tau,1)\, d\tau, \tag{4.15}$$

$$D_{k\ell}^{\pm} = \frac{1}{2}\int_{-1}^{1}\int_{-1}^{1} \left[\psi_{,t}^{(k)} \pm \nu\psi_{,\xi}^{(k)}\right]\psi^{(\ell)}\, d\xi\, d\tau. \tag{4.16}$$

If we take $M = 1$, we arrive at the first-order scheme:

$$W_{1i}^{n+1} - W_{1i}^{n} - \nu W_{1\,i+1}^{n+1} + \nu W_{1i}^{n+1} = \alpha\left(W_{2i}^{n+1} - W_{1i}^{n+1}\right), \tag{4.17}$$

$$W_{2i}^{n+1} - W_{2i}^{n} + \nu W_{2\,i}^{n+1} - \nu W_{2\,i-1}^{n+1} = \alpha\left(W_{1i}^{n+1} - W_{2i}^{n+1}\right). \tag{4.18}$$

This can be rewritten as

$$(1+\alpha+\nu)W_{1i}^{n+1} - \alpha W_{2i}^{n+1} - \nu W_{1\,i+1}^{n+1} = W_{1i}^{n}, \tag{4.19}$$

$$(1+\alpha+\nu)W_{2i}^{n+1} - \alpha W_{1i}^{n+1} - \nu W_{2\,i-1}^{n+1} = W_{2i}^{n}. \tag{4.20}$$

If we assume periodic boundary conditions, we arrive at the following $(2m_x)\times(2m_x)$ linear system:

$$\left[\begin{array}{cccccc:cccccc}
\beta & -\nu & & & & & -\alpha & & & & & \\
 & \beta & -\nu & & & & & -\alpha & & & & \\
 & & \ddots & \ddots & & & & & \ddots & & & \\
 & & & \beta & -\nu & & & & & -\alpha & & \\
-\nu & & & & \beta & & & & & & -\alpha & \\
\hdashline
-\alpha & & & & & & \beta & & & & & -\nu \\
 & -\alpha & & & & & -\nu & \beta & & & & \\
 & & \ddots & & & & & \ddots & \ddots & & & \\
 & & & -\alpha & & & & & -\nu & \beta & & \\
 & & & & -\alpha & & & & & -\nu & \beta &
\end{array}\right]
\left[\begin{array}{c} W_{11}^{n+1} \\ W_{12}^{n+1} \\ \vdots \\ W_{1\,m_x-1}^{n+1} \\ W_{1\,m_x}^{n+1} \\ \hdashline W_{21}^{n+1} \\ W_{22}^{n+1} \\ \vdots \\ W_{2\,m_x-1}^{n+1} \\ W_{2\,m_x}^{n+1} \end{array}\right]
=
\left[\begin{array}{c} W_{11}^{n} \\ W_{12}^{n} \\ \vdots \\ W_{1\,m_x-1}^{n} \\ W_{1\,m_x}^{n} \\ \hdashline W_{21}^{n} \\ W_{22}^{n} \\ \vdots \\ W_{2\,m_x-1}^{n} \\ W_{2\,m_x}^{n} \end{array}\right], \tag{4.21}$$

where

$$\beta = 1 + \alpha + \nu = 1 + \Delta t\left(\frac{\sigma\Delta x + 2\varepsilon}{2\varepsilon^2\Delta x}\right). \tag{4.22}$$

## 4.1 Stability of first-order scheme

We can rewrite the first order scheme (4.19)–(4.20) as

$$A\begin{bmatrix} W_{1j}^{n+1} \\ W_{2j}^{n+1} \end{bmatrix} + B\begin{bmatrix} W_{1\ j+1}^{n+1} \\ W_{2\ j+1}^{n+1} \end{bmatrix} + C\begin{bmatrix} W_{1\ j-1}^{n+1} \\ W_{2\ j-1}^{n+1} \end{bmatrix} = \begin{bmatrix} W_{1j}^{n} \\ W_{2j}^{n} \end{bmatrix}, \tag{4.23}$$

where the matrices $A$, $B$, and $C$ are defined:

$$A = \begin{bmatrix} 1+\alpha+\nu & -\alpha \\ -\alpha & 1+\alpha+\nu \end{bmatrix}, \qquad B = \begin{bmatrix} -\nu & 0 \\ 0 & 0 \end{bmatrix}, \qquad C = \begin{bmatrix} 0 & 0 \\ 0 & -\nu \end{bmatrix}. \tag{4.24}$$

Now we use the ansatz $\begin{bmatrix} W_{1j}^{n+1} \\ W_{2j}^{n+1} \end{bmatrix} = G^{n+1}e^{imj\Delta x}$ in (4.23) to get

$$AG^{n+1}e^{imj\Delta x} + BG^{n+1}e^{im(j+1)\Delta x} + CG^{n+1}e^{im(j-1)\Delta x} = G^n e^{imj\Delta x}. \tag{4.25}$$

After right-multiplying (4.25) by $[G^n]^{-1}e^{-imj\Delta x}$ on both sides, we have

$$AG + BGe^{im\Delta x} + CGe^{-im\Delta x} = I. \tag{4.26}$$

Hence

$$G^{-1} = A + Be^{im\Delta x} + Ce^{-im\Delta x} \tag{4.27}$$

$$= \begin{bmatrix} 1+\alpha+\nu(1-e^{im\Delta x}) & -\alpha \\ -\alpha & 1+\alpha+\nu(1-e^{-im\Delta x}) \end{bmatrix}. \tag{4.28}$$

Let $c$ be the determinant of $A + Be^{im\Delta x} + Ce^{-im\Delta x}$, which is given by

$$c = [1+\alpha+\nu(1-e^{im\Delta x})][1+\alpha+\nu(1-e^{-im\Delta x})] - \alpha^2. \tag{4.29}$$

We can see that $c$ is non-zero and well-defined for $\Delta x$ not equal to zero, so we have

$$G = \frac{1}{c}\begin{bmatrix} 1+\alpha+\nu(1-e^{-im\Delta x}) & \alpha \\ \alpha & 1+\alpha+\nu(1-e^{im\Delta x}) \end{bmatrix}. \tag{4.30}$$

We wish to calculate $\|G\|_2 = \sqrt{\rho(G^*G)}$, where $\rho(G^*G)$ is the spectral radius of the matrix $G^*G$. The eigenvalues of $G^*G$ are

$$\lambda_1 = \frac{2\nu\beta(1-\cos(m\Delta x)) + 1 + 2\alpha + 2\alpha^2 - 2\alpha\sqrt{(\alpha+1)^2 + 2\nu\beta(1-\cos(m\Delta x))}}{(1+2\alpha+2\nu\beta(1-\cos(m\Delta x)))^2}, \tag{4.31}$$

$$\lambda_2 = \frac{2\nu\beta(1-\cos(m\Delta x)) + 1 + 2\alpha + 2\alpha^2 + 2\alpha\sqrt{(\alpha+1)^2 + 2\nu\beta(1-\cos(m\Delta x))}}{1+2\alpha+2\nu\beta(1-\cos(m\Delta x)))^2}. \tag{4.32}$$

For $\Delta x$ sufficiently small, $1-\cos(m\Delta x) \approx 0$, so we can ignore this term. We wish to show that $|\lambda_1|, |\lambda_2| \leq 1$.

$$|\lambda_1| = \frac{1+2\alpha+2\alpha^2-2\alpha(\alpha+1)}{(1+2\alpha)^2} \tag{4.33}$$

$$= \frac{1}{(1+2\alpha)^2} \tag{4.34}$$

$$\leq 1, \tag{4.35}$$

and similarly for $\lambda_2$,

$$|\lambda_2| = \frac{1+2\alpha+2\alpha^2+2\alpha(\alpha+1)}{(1+2\alpha)^2} \tag{4.36}$$

$$= \frac{1+4\alpha+4\alpha^2}{1+4\alpha+4\alpha^2} \tag{4.37}$$

$$= 1. \tag{4.38}$$

Hence the spectral radius $\rho(G^*G) \leq 1$, so $\|G\|_2 \leq 1$. Then $\|G^n\|_2 \leq \|G\|_2^n \leq 1^n = 1$, therefore the first order scheme is stable. Further, there is no restriction on $\Delta x$ or $\Delta t$, so this scheme is unconditionally stable.

## 4.2 Predictor-corrector space-time DG method

The space-time discontinuous Galerkin method described above is a first-order method which is slow to converge. When $\sigma = 0$, the scheme is equivalent to a backward Euler

method for the advection equation. To improve the accuracy of this method, we employ the implicit space-time scheme as a predictor method and correct the solution with an explicit space-time discontinuous Galerkin scheme.

Since the predictor method gives a piece-wise constant representation of the solution in each space-time cell, we apply the method twice with different values of $\Delta t$ and interpolate on four quadrature points in each cell to get a bilinear function which varies in space and time.

We first carry out the predictor method with a time-step

$$\Delta t_1 = \frac{\Delta t(1-\sqrt{3})}{2}, \tag{4.39}$$

and solve the resulting linear system as in (4.21) with

$$\begin{aligned} \nu_1 &= \frac{\Delta t_1}{\varepsilon \Delta x}, \\ \alpha_1 &= \frac{\sigma \Delta t_1}{2\varepsilon^2}, \\ \beta_1 &= 1 + \alpha_1 + \nu_1. \end{aligned} \tag{4.40}$$

We then use the predictor method again, this time with the time step

$$\Delta t_2 = \frac{\Delta t(1+\sqrt{3})}{2}. \tag{4.41}$$

Our goal is to interpolate on the values of the solution achieved after each predictor step. Since we are only marching forward in time with constant values in each cell, we need to add spatial variation to our interpolant. Hence we consider the values of the predicted solution after the first predictor step in cells $x_{i-1}$, $x_i$, and $x_{i+1}$.

We interpolate on these three points to get a quadratic polynomial of the form

$$\hat{u}(x) = \alpha_0 + \alpha_1 x + \alpha_2 x^2. \tag{4.42}$$

Then we write this polynomial in terms of $\xi$, where $x = x_i + \xi(\Delta x/2)$, by

$$\hat{u}(\xi) = \alpha_0 + \alpha_1 \left( x_i + \xi \frac{\Delta x}{2} \right) + \alpha_2 \left( x_i + \xi \frac{\Delta x}{2} \right)^2. \tag{4.43}$$

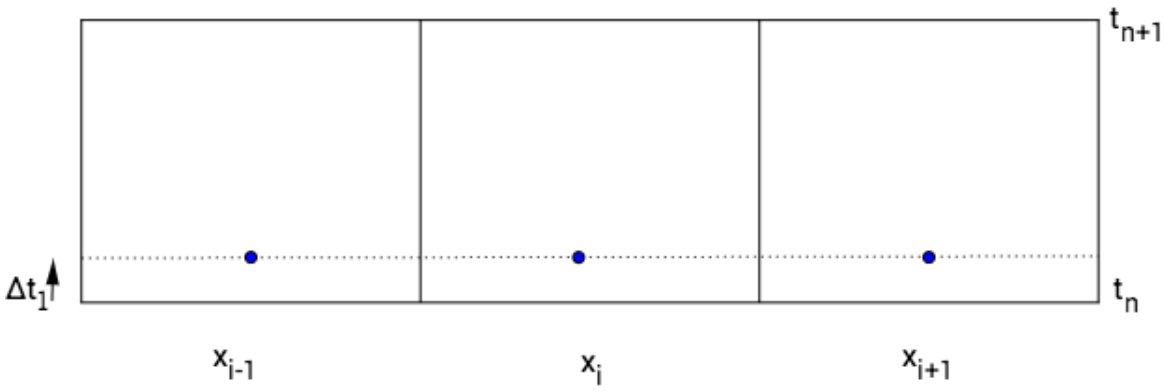


Figure 4.1 First predictor step

We evaluate $\hat{u}$ at $\xi = \pm\frac{1}{\sqrt{3}}$. Then we repeat this process with the second predictor step using $\Delta t_2$. Now we have four values in each space time cell at the Gaussian quadrature points

$$(\tau, \xi) \in \left\{ \left( -\frac{1}{\sqrt{3}}, -\frac{1}{\sqrt{3}} \right), \left( -\frac{1}{\sqrt{3}}, \frac{1}{\sqrt{3}} \right), \left( \frac{1}{\sqrt{3}}, -\frac{1}{\sqrt{3}} \right), \left( \frac{1}{\sqrt{3}}, \frac{1}{\sqrt{3}} \right) \right\}. \tag{4.44}$$

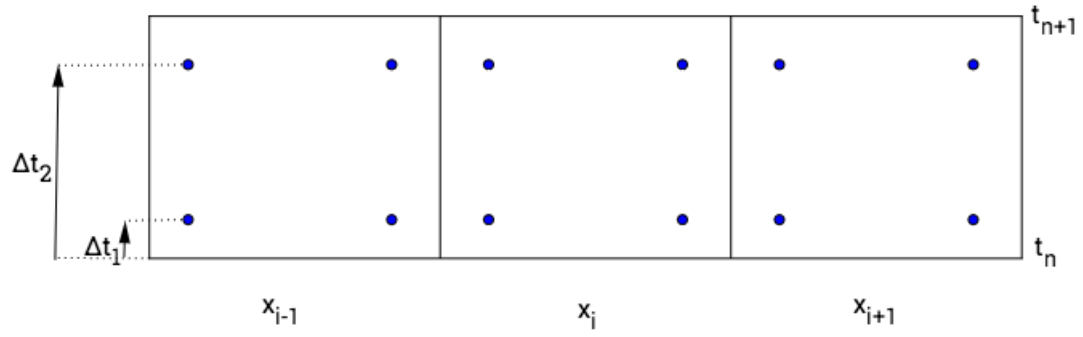


Figure 4.2 Space-time cell quadrature points

We interpolate on these four points to get a bilinear function on each cell of the form

$$\tilde{u}(\tau,\xi) = a_0 + \sqrt{3}a_1\xi + \sqrt{3}a_2\tau + 3a_3\xi\tau. \tag{4.45}$$

We use (4.45) in place of our Galerkin expansion in the space-time DG corrector step, which is described below.

The conservation form of our characteristic system (4.2) is written,

$$u_{,\tau} + Au_{,\xi} = s(u), \tag{4.46}$$

where

$$u = \begin{pmatrix} w_1 \\ w_2 \end{pmatrix}, \quad A = \begin{pmatrix} -\nu & 0 \\ 0 & \nu \end{pmatrix}, \quad s(u) = \frac{\alpha}{2}\begin{pmatrix} w_2 - w_1 \\ w_1 - w_2 \end{pmatrix}. \tag{4.47}$$

We integrate (4.46) with respect to $\xi$ and $\tau$ against the spatial basis functions

$$\phi^{(\ell)}(\tau,\xi) \in \left\{1, \sqrt{3}\xi, \frac{\sqrt{5}}{2}(3\xi^2-1), \dots\right\}, \tag{4.48}$$

and plug in our ansatz from interpolating on the four space-time Gaussian quadrature points. Then we have

$$U_i^{(\ell)n+1} - U_i^{(\ell)n} + \frac{1}{2}A\int_{-1}^{1}\int_{-1}^{1}\tilde{u}_{,\xi}\phi^{(\ell)}\,d\tau d\xi = \frac{\alpha}{4}\int_{-1}^{1}\int_{-1}^{1}s(\tilde{u})\,d\tau d\xi. \tag{4.49}$$

Next, we integrate by parts. In terms of the characteristic variables $w_1$ and $w_2$, we have

$$\begin{aligned} W_{1i}^{(\ell)n+1} &= W_{1i}^{(\ell)n} + \frac{\nu}{2}\int_{-1}^{1}\left[\tilde{w}_1\phi^{(\ell)}\Big|_{\xi=-1}^{\xi=1} - \int_{-1}^{1}\tilde{w}_1\phi_{,\xi}^{(\ell)}\,d\xi\right]d\tau \\ &\quad + \frac{\alpha}{4}\int_{-1}^{1}\int_{-1}^{1}(\tilde{w}_2 - \tilde{w}_1)\phi^{(\ell)}\,d\xi d\tau, \\ W_{2i}^{(\ell)n+1} &= W_{2i}^{(\ell)n} - \frac{\nu}{2}\int_{-1}^{1}\left[\tilde{w}_2\phi^{(\ell)}\Big|_{\xi=-1}^{\xi=1} - \int_{-1}^{1}\tilde{w}_2\phi_{,\xi}^{(\ell)}\,d\xi\right]d\tau \\ &\quad + \frac{\alpha}{4}\int_{-1}^{1}\int_{-1}^{1}(\tilde{w}_1 - \tilde{w}_2)\,d\xi d\tau. \end{aligned} \tag{4.50}$$

For the boundary terms, we use an upwind flux since the value of $\tilde{w}_1$ and $\tilde{w}_2$ are not defined for $\xi = \pm 1$. After evaluating the integrals for $\ell = 1, 2, \dots, M(M+1)/2$, we have an explicit scheme for $U_i^{(\ell)n+1}$.

This scheme is first order in time and space and admits the CFL condition

$$\frac{\Delta t}{\varepsilon \Delta x} \leq 1. \tag{4.51}$$

The dependence of the CFL number on $\varepsilon$ means that the corrector method is not asymptotic preserving. The CFL limit arises from the explicit nature of the method. In future work, we can achieve asymptotic preservation by modifying this scheme to include some implicit treatment and eliminate or at least relax the CFL restriction.

# CHAPTER 5. NUMERICAL RESULTS

In this chapter we present the convergence results and plots for our space-time DG predictor-corrector method and comment on the results. In all cases, we use a smooth Gaussian pulse for the initial data and assume periodic boundary conditions. We compare these numerical methods against a high order spectral method which is used as a proxy for an exact solution.

## 5.1 Convergence results

We first consider the space-time DG method alone, without the correction step. The convergence study was carried out on the interval $[-1, 1]$ with periodic boundary conditions and $\varepsilon = 1$. All error analysis and plots were created for the density

$$\rho = w_1 + w_2. \tag{5.1}$$

Table 5.1 Convergence study for predictor method with $\varepsilon = 1$.

| $\Delta t$ | $\Delta x$ | Relative $L^2$ Error | Error Ratio | Order |
|---|---|---|---|---|
| 0.0500 | 0.0500 | 6.927419071030023e-01 | | |
| 0.0250 | 0.0250 | 5.712003278315951e-01 | 1.212782754752271e+00 | 0.6064 |
| 0.0125 | 0.0125 | 4.365133600138014e-01 | 1.308551765319475e+00 | 0.6543 |
| 0.0063 | 0.0063 | 3.035954727360871e-01 | 1.437812481457056e+00 | 0.7189 |
| 0.0031 | 0.0031 | 1.912190109781601e-01 | 1.587684567465742e+00 | 0.7938 |
| 0.0016 | 0.0016 | 1.105202670256767e-01 | 1.730171452931207e+00 | 0.8651 |
| 7.8125e-04 | 7.8125e-04 | 6.005532722393999e-02 | 1.840307465373693e+00 | 0.9202 |

This method is first order, but it converges slowly. When combined with the correction step, we see from Table 5.2 that the relative $L^2$ error decreases.

Table 5.2 Convergence study for predictor-corrector method with $\varepsilon = 1$.

| $\Delta t$ | $\Delta x$ | Relative $L^2$ Error | Error Ratio | Order |
|---|---|---|---|---|
| 0.0500 | 0.0500 | 4.485023186602793e-01 | | |
| 0.0250 | 0.0250 | 2.884198497655510e-01 | 1.555032772622464e+00 | 0.7775 |
| 0.0125 | 0.0125 | 1.784092132906744e-01 | 1.616619705035306e+00 | 0.8083 |
| 0.0063 | 0.0063 | 1.073144768680213e-01 | 1.662489707796719e+00 | 0.8312 |
| 0.0031 | 0.0031 | 6.527492747208395e-02 | 1.644038239857353e+00 | 0.8220 |
| 0.0016 | 0.0016 | 4.265586064802572e-02 | 1.530268677748626e+00 | 0.7651 |
| 7.8125e-04 | 7.8125e-04 | 3.141457362437822e-02 | 1.357836689367768e+00 | 0.6789 |

The correction method does reduce the error significantly, but it is still very slow to converge. Machine error overtakes the numerical error before the scheme realizes first order convergence. In Figure 5.1, we choose $\varepsilon = 1$, $\Delta x = 0.0125$, and $\Delta t = \Delta x$. The predictor solution is represented by the blue 'x', and the spectral method is represented by the green 'o'. We use the same parameters in Figure 5.2, where we plot the predictor-corrector method solution against the spectral solution as well.

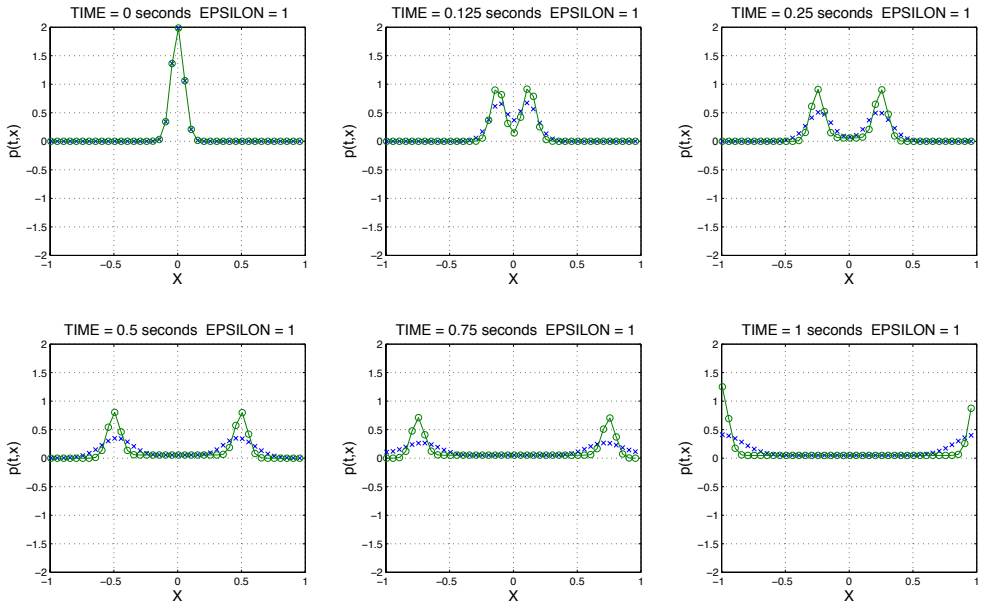


Figure 5.1 Plot of predictor method in rarefied regime.

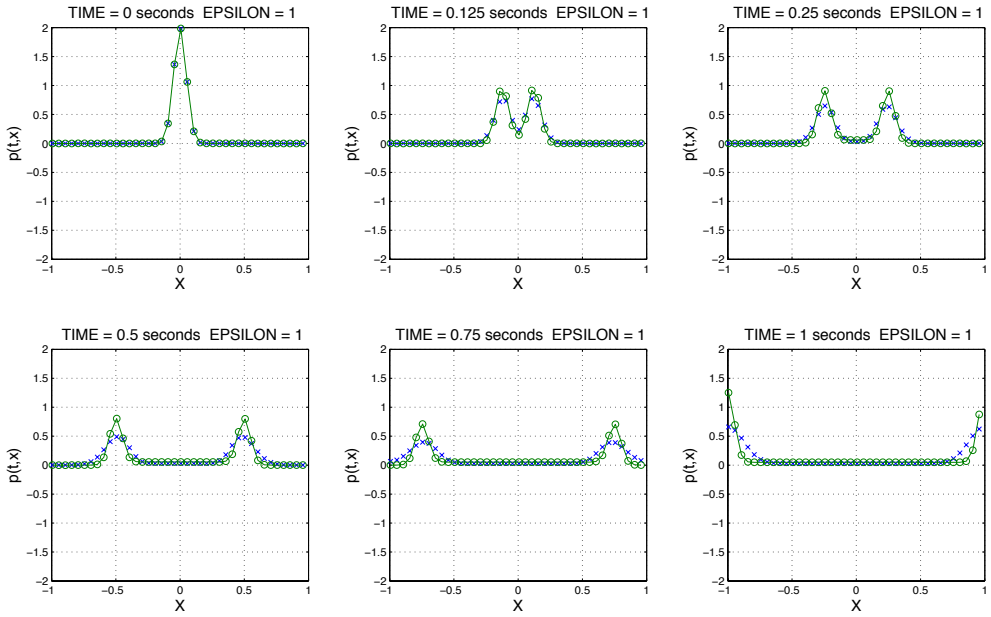


Figure 5.2 Plot of predictor-corrector method in rarefied regime.

We can see that the corrector does increase the amplitude of the solution to more closely match the actual solution, but there is still numerical diffusion present.

We also test the schemes in the diffusive regime using $\varepsilon = 0.01$.

Table 5.3 Convergence study for predictor method with $\varepsilon = 0.01$.

| $\Delta t$ | $\Delta x$ | Relative $L^2$ Error | Error Ratio | Order |
|---|---|---|---|---|
| 0.0500 | 0.0500 | 2.127718789783104e-01 | | |
| 0.0250 | 0.0250 | 1.487998429996711e-01 | 1.429920050243472e+00 | 0.7150 |
| 0.0125 | 0.0125 | 9.119695898870370e-02 | 1.631631631687440e+00 | 0.8158 |
| 0.0063 | 0.0063 | 5.117550322821975e-02 | 1.782043228417437e+00 | 0.8910 |
| 0.0031 | 0.0031 | 2.722589719354912e-02 | 1.879662692634615e+00 | 0.9398 |
| 0.0016 | 0.0016 | 1.405952244695035e-02 | 1.936473823792976e+00 | 0.9682 |
| 7.8125e-04 | 7.8125e-04 | 7.146539686555572e-03 | 1.967318879289207e+00 | 0.9837 |

In the diffusive regime, the predictor method converges more quickly than in the rarefied regime. The full predictor-corrector method is less accurate in the diffusive regime. In Figure 5.3, we can see that the solution for the full scheme seems to diffusive more quickly than the high order spectral solution. This leads to the low order that we see in Table 5.4.

Table 5.4 Convergence study for predictor-corrector method with $\varepsilon = 0.01$.

| $\Delta t$ | $\Delta x$ | Relative $L^2$ Error | Error Ratio | Order |
|---|---|---|---|---|
| 0.0500 | 0.0500 | 3.016334068977755e-01 | | |
| 0.0250 | 0.0250 | 2.620047523299200e-01 | 1.151251663244469e+00 | 0.5756 |
| 0.0125 | 0.0125 | 2.238268367253313e-01 | 1.170568981642888e+00 | 0.5853 |
| 0.0063 | 0.0063 | 1.981398894291084e-01 | 1.129640464473022e+00 | 0.5648 |
| 0.0031 | 0.0031 | 1.832265712027665e-01 | 1.081392770319531e+00 | 0.5407 |
| 0.0016 | 0.0016 | 1.751733374370372e-01 | 1.045972942478326e+00 | 0.5230 |
| 7.8125e-04 | 7.8125e-04 | 1.709849999960885e-01 | 1.024495350124540e+00 | 0.5122 |

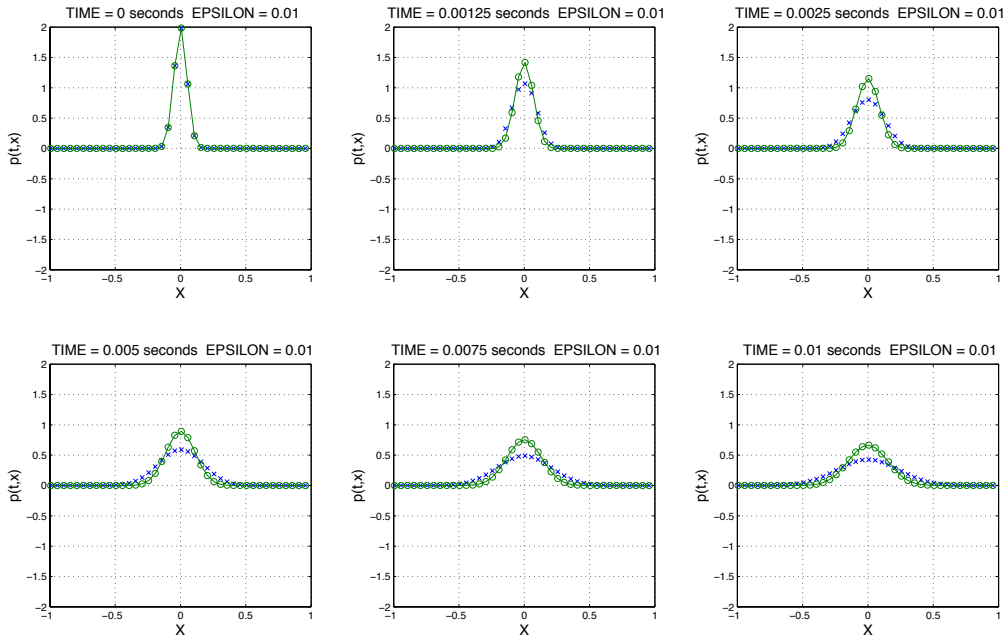


Figure 5.3 Plots of full precitor-corrector scheme in diffusive regime.

## 5.2 Concluding remarks and future work

The corrector method presented in Chapter 4 is asymptotic preserving, as it is unconditionally stable and maintains first order accuracy as $\varepsilon \to 0^+$. Because this is a fully implicit method, it behaves well in the diffusive regime, where the domain of the dependence of the hyperbolic heat equation becomes the entire real line. It is less accurate in the rarefied regime, although it does eventually achieve first order accuracy.

Our predictor-corrector method does not appear to be asymptotic preserving due to the time step restriction

$$\frac{\Delta t}{\varepsilon \Delta x} \leq 1. \tag{5.2}$$

Since the predictor method is unconditionally stable, the CFL condition arises from the corrector step. This restriction is due to the explicit treatment of the source coupling terms, which had been treated implicitly in our predictor method, as well as in the

methods of Shi Jin [12] and McClarren, *et al.* [16].

In the future, we would like to modify our corrector step so that we can achieve unconditionally stability, which would result in an asymptotic preserving scheme. Then we will easily be able to extend the method to higher dimensions as well as to more complicated systems, such as the $P_N$ equations for $N > 1$.

# BIBLIOGRAPHY

[1] Aristov, V.V. (2001). *Direct Methods for Solving the Boltzmann Equation and Study of Nonequilibrium Flows*. Dprdrecht: Kluwer Academic Publishers.

[2] Arnold, D.N.; Brezzi, F.; Cockburn, B.; Marini, L. D., Unified analysis of discontinuous Galerkin methods for elliptic problems. *SIAM J. Numer. Anal.*, 39 (2002), no. 5, 1749–1779.

[3] Bassi, F. and Rebay, S., A high-order accurate discontinuous finite element method for the numerical solution of the compressible Navier-Stokes equations. *J. Comput. Phys.,* 131 (1997), 267–279.

[4] Cockburn, B., Discontinuous Galerkin Methods. *ZAMM J. of App. Math. and Mech.,* 83 (2003), no. 11, 731–754.

[5] Cockburn, B.; Karniadakis, G.E.; Shu, C.-W., (2000) *Discontinuous Galerkin Methods*. Berlin: Springer.

[6] Cockburn, B. and Shu, C.-W., The Runge-Kutta local projection P1-discontinuous Galerkin finite element method for scalar conservation laws. *Mathematical Modeling and Numerical Analysis,* 25 (1991), 337–361.

[7] Goldstein, S., On diffusion by discontinuous movements, and on the telegraph equation. *Quart. J. Mech. Appl. Math.,* 4 (1951), 129–156.

[8] Gosse, L. and Toscani, G., An asymptotic-preserving well-balanced scheme for the hyperbolic heat equations. *C.R. Acad. Sci. Paris*, Ser. I 334 (2002), 337–342.

[9] Hauck, C. D. and Lowrie, Robert B., Temporal regularization of the $P_N$ equations. *SIAM Multiscale Modeling and Simulation*. 7 (2009), no. 4, 1497–1524.

[10] Hesthaven, Jan S. and Warburton, T. (2008). *Nodal Discontinuous Galerkin Methods: Algorithms, Analysis, and Applications*. New York City: Springer.

[11] Jamet, P. Galerkin-type approximations which are discontinuous in time for parabolic equations in a variable domain. *SIAM J. Numer. Anal.,* 15 (1978), 912–928.

[12] Jin, S., Efficient asymptotic-preserving (AP) schemes for some multiscale kinetic equations. *SIAM J. Sci. Comput.* 21 (1999), no. 2, 441–454.

[13] Jin, S.; Pareschi, L.; Toscani, G., Uniformly accurate diffusive relaxation schemes for multiscale transport equations. *SIAM J. Numer. Anal.* 38 (2000), no. 3, 913–936.

[14] LeSaint, P. and Raviart, P.A., On a finite element method for solving the neutron transport equation. In C. de Boor, editor, *Mathematical aspects of finite elements in partial differential equations*, 89–145. Academic Press (1974).

[15] Lions, P. L. and Toscani, G., Diffusive limit for finite velocity Boltzmann kinetic models. *Revista Matematica Iberoamericana* 13 (1997), no. 3, 473–513.

[16] McClarren, R. G.; Evans, T. M.; Lowrie, R. B.; Densmore, J. D., Semi-implicit time integration for $P_N$ thermal radiative transfer. *J. Comput. Phys.* 227 (2008), no. 16, 7561–7586.

[17] Reed, W.H. and Hill, T.R., Triangular mesh methods for the neutron transport equation. *Technical Report* LA-UR-73-479, Los Alamos Scientific Laboratory, (1973).

[18] Ruijgrok, W. and Wu, T.T., A completely solvable model of the nonlinear Boltzmann equation, *Phys. A,* 113 (1982), 401–416.

[19] Taylor, G.I., Diffusion by continuous movements. *Proc. London Math. Soc.,* 20 (1921), 196–212.